# Salt Effect in Ion-Pair Dynamics after Bimolecular Photoinduced Electron Transfer in a Room-Temperature Ionic Liquid

Arnulf Rosspeintner,[†] Marius Koch,[†,§] Gonzalo Angulo,*,[‡] and Eric Vauthey*,[†]

[†]Department of Physical Chemistry, University of Geneva, 30 quai Ernest-Ansermet, CH-1211 Geneva, Switzerland
[‡]Institute of Physical Chemistry, Polish Academy of Sciences, 01-224 Warsaw, Poland

S *Supporting Information*

ABSTRACT: Bimolecular photoinduced electron transfer between perylene and two quenchers was investigated in an imidazolium room-temperature ionic liquid (RTIL) and in a dipolar solvent mixture of the same viscosity using transient absorption on the subpicosecond to submicrosecond time scales. Whereas charge separation dynamics were similar in both solvents, significant differences were observed in the temporal evolution of the ensuing radical ions: although small, the free-ion yield is significantly larger in the RTIL, and recombination of the ion pair to the triplet state of perylene is more efficient in the dipolar solvent. The temporal evolution of reactant, ion, and triplet state populations could be well reproduced using unified encounter theory. This analysis reveals that the observed differences can be explained by the strong screening of the Coulomb potential in the ion pair by the ionic solvent. In essence, RTILs favor free ions compared to highly dipolar solvents of the same viscosity.
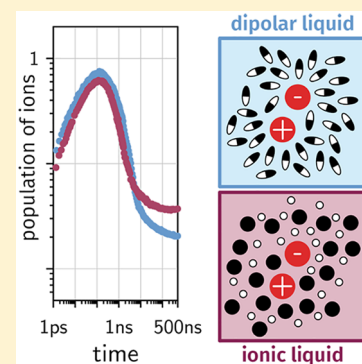
Room-temperature ionic liquids (RTILs) are attracting considerable attention because several of their properties make them promising solvents for a wide range of applications.[1−4] Substantial effort is being invested to understand how the ionic nature of these liquids affects chemical reactivity compared to conventional solvents.[5−12] Reactions involving charged species/intermediates could be expected to be significantly affected when going to RTILs. Photoinduced electron-transfer (ET) reactions are well suited to address this question, not only because their dynamics can be monitored with high time resolution but also because of the deep understanding of these processes achieved so far in conventional solvents.[13−15] The dynamics of photoinduced intramolecular charge-transfer processes were found not to be so much affected by the ionic nature of the RTILs as by their high viscosity.[16−24] Because of this high viscosity, the dynamics of bimolecular photoinduced ET in RTILs are strongly nonexponential and dominated by static quenching and transient effects. Several investigations, where these effects were properly accounted for, revealed that the dynamics in RTILs were similar to those in dipolar solvents of the same viscosity.[25−29] Bimolecular photoinduced ET between neutral reactants, i.e., charge separation (CS), produces ion pairs, which either dissociate into free ions or recombine. As one of the main applications of these reactions is the generation of free ions, the parameters that affect their production in conventional solvents have been thoroughly investigated.[30−33] Addition of an inert salt was found to often enhance the free ion yield and/or to slow down the recombination of free ions.[34−38] This was usually explained by the special salt effect, namely, the rapid exchange between the inert salt and the ion pairs.[39] Consequently, RTILs can be anticipated to be favorable media for the photoproduction of ions.
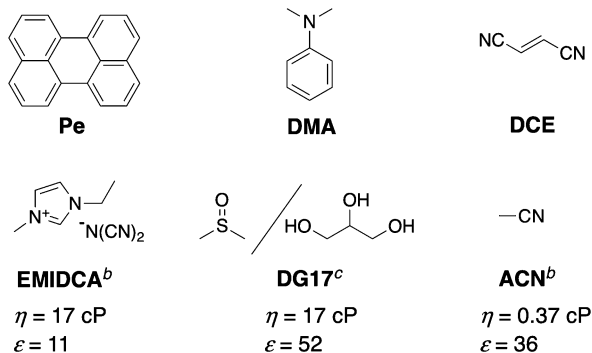
Surprisingly, very little is known about ion-pair dynamics upon bimolecular photoinduced CS in RTILs. The free-ion yield with the pyrene/dimethylaniline pair was reported to drop from 50% in acetonitrile to 1.5% in a 34 cP RTIL.[40] More recently, very slow escape of ion pairs to free ions was deduced from magnetic field effect measurements in a 73 cP RTIL.[41] However, the limited time resolution did not allow monitoring the entire temporal evolution of the ion pairs. These investigations suggest that RTILs are poor solvents for producing free ions upon bimolecular photoinduced CS. However, these results in RTILs were not compared with those in a dipolar solvent of similar viscosity. Therefore, the effects due to the ionic nature of RTILs could not be disentangled from those related to their high viscosity.

We investigated the photoinduced ET between perylene (Pe) in the S_1 state and either an electron donor (*N,N*-dimethylaniline, DMA) or an electron acceptor (dicyanoethylene, DCE) in a 17 cP imidazolium-based RTIL (EMIDCA), in a dimethyl sulfoxide (DMSO)/glycerol mixture of the same viscosity (DG17),[42] and in acetonitrile (ACN, Chart 1). By using electronic transient absorption (TA) spectroscopy on a 0−500 ns temporal window with a 100 fs time resolution,[43] the different populations involved in the reaction could be clearly distinguished and monitored up to the stage where the ions are free.
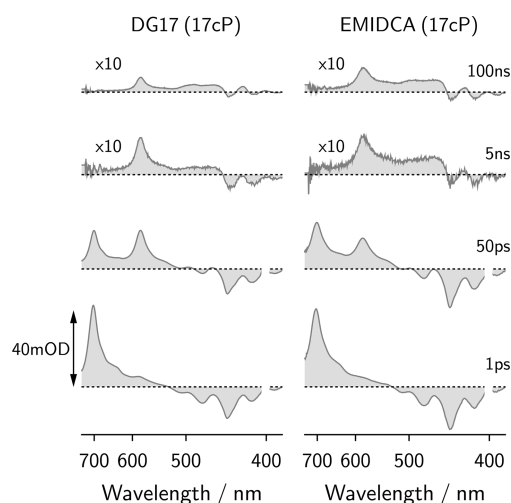
Chart 1. Fluorophore, Quenchers, and Solvents[a]

Pe   **DMA**   **DCE**

EMIDCA[b]   **DG17**[c]   **ACN**[b]

$\eta = 17$ cP $\eta = 17$ cP $\eta = 0.37$ cP
$\varepsilon = 11$ $\varepsilon = 52$ $\varepsilon = 36$

[a]η: viscosity. ε: dielectric constant. [b]From ref 26. [c]From ref 42.

Figure 1. Selected transient absorption spectra measured with Pe and 0.37 M DMA in DG17 and EMIDCA at different time delays after excitation at either 400 nm (1 and 50 ps) or 355 nm (5 and 100 ns).

Representative TA spectra recorded with Pe/DMA in DG17 and EMIDCA are shown in Figure 1. The earliest ones are dominated by the excited-state absorption band of ^{1}Pe* around 700 nm and by the stimulated emission and ground-state bleach below 520 nm. At intermediate times, the 580 nm band of Pe$^{\bullet-}$ is also visible. The radical cation of the quencher, DMA$^{\bullet+}$, absorbs around 480 nm, but its absorbance is

significantly smaller than that of Pe$^{\bullet-}$.[44] After a few nanoseconds, the ^{1}Pe* band has entirely decayed, whereas the Pe$^{\bullet-}$ band is still visible. Additionally, a new band between 520 and 450 nm due to Pe in the triplet state, ^{3}Pe*, is visible. The same spectral features were observed in ACN (Figure S6) and at other DMA concentrations (0.19, 0.63, and 0.87 M). In the presence of DCE (0.23 and 0.72 M) instead of DMA, the direction of CS is reversed and the Pe$^{\bullet-}$ band is replaced by that of Pe$^{\bullet+}$ at 540 nm (Figure S7). In this case, the ^{3}Pe* band is not observed.

The contributions of ^{1}Pe* (S), Pe$^{\bullet\pm}$ (I), and ^{3}Pe* (T) to the TA spectra were determined using the model-free method described in ref 44 to obtain the temporal evolution of their relative population, $P^x(t)$ (x = S, I, T) (see the Supporting Information for details). The time profiles at 0.63 M DMA and 0.72 M DCE in all three solvents are depicted in Figure 2, whereas those at the other concentrations are shown in Figures S8−13.

These figures reveal that the decays of $P^S(t)$, due mostly to CS, are similar in both EMIDCA and DG17, as previously observed with another donor/acceptor pair.[26] As expected for a diffusion-assisted process, it is much slower in these 17 cP solvents than in ACN. Whereas $P^S(t)$ does not exhibit a pronounced dependence on the nature of the quencher, the ion population, $P^I(t)$, decays faster with DCE than with DMA. This difference can be explained by the smaller driving force for charge recombination with DCE and by considering that this process occurs in the Marcus inverted region.[45] With the exception of Pe/DCE in DG17, $P^I(t)$ does not decay entirely to zero within the experimental time window but levels off at a residual value that corresponds to the free-ion population. As their bulk recombination occurs on a longer time scale, this residual $P^I(t)$ value is a good measure of the free-ion yield, Φ_I.

For Pe/DCE, Φ_I amounts to about 2% in ACN, as also found previously,[46] and to ~1.5% in EMIDCA, whereas it is negligibly small in DG17. For Pe/DMA, Φ_I is around 50% in ACN, 3−4% in EMIDCA and 1−2% in DG17. As expected, high viscosity impedes the escape of the ions from the pairs. However, these results reveal that this effect is less pronounced in an ionic liquid. Although small, the free-ion yield in EMIDCA is twice as large as in a dipolar solvent of the same viscosity.

The ^{3}Pe* population appears a few nanoseconds after excitation and rises up to a maximum yield, Φ_T, that is the
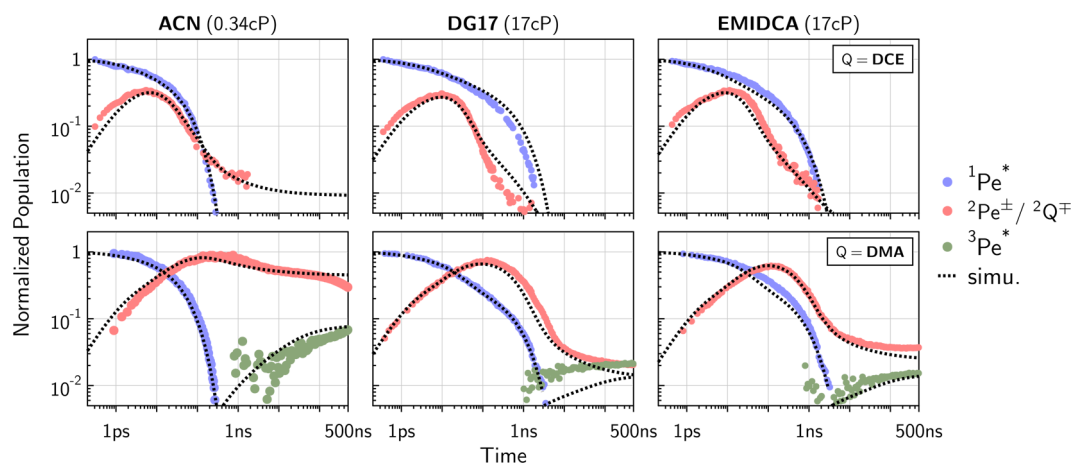
**Figure 2.** Measured and simulated time evolutions of the populations of ^{1}Pe*, Pe$^{\bullet\pm}$, and ^{3}Pe* with 0.72 M DCE (top) and 0.63 M DMA (bottom).

largest in ACN, around 8%, and decreases to 2−3% in DG17 and 1−2% in EMIDCA. This population is due to the recombination of ion pairs in the triplet state, themselves generated upon spin conversion of the singlet ion pairs produced originally.[47] For spin conversion to be operative, the ions should be sufficiently distant for the exchange energy to be negligible and, thus, for the singlet and triplet states to be nearly degenerate. As a consequence, triplet recombination occurs mostly at remote distance and/or upon reencounter of the triplet ion pairs. The higher triplet yield in ACN can be attributed to the low viscosity of this solvent that facilitates ion diffusion. For a given donor/acceptor pair, Φ_I and Φ_T should correlate, because spin conversion occurs on the way to the free ions. Such correlation was indeed observed with Pe/DMA in a series of dipolar solvents of increasing viscosity.[44] Here, however, the triplet yield is smaller in EMIDCA than in DG17, despite a higher free-ion yield.

To get deeper insight into the origin of these different Φ_I and Φ_T in EMIDCA and DG17, the $P^x(t)$ (x = S, I, T) profiles were analyzed using the unified encounter theory (UET).[44,48] All details of this approach have been described previously for the Pe/DMA pair in dipolar solvents,[44] and only its most important aspects are discussed here (see also Supporting Information). This analysis is based on reaction Scheme 1 and

Scheme 1. Reaction Scheme Used for Simulating the Measured Population Profiles, $P^x(t)$ with x = S, I , T[a]
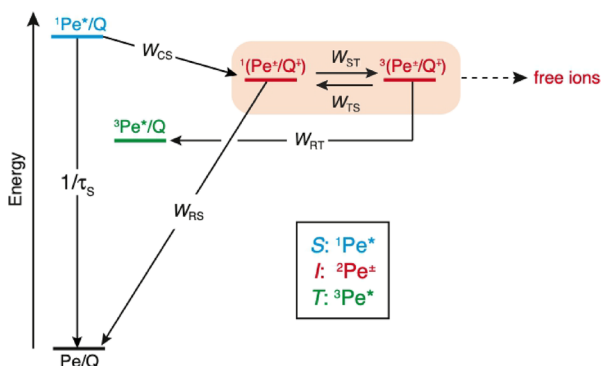
[a]The formation of free ions is intrinsically accounted for in the model. Their bulk recombination is not considered, because it does not take place within the time window of the measurements as shown previously.[44]

considers the time dependence of the reactant and ion-pair distribution functions, $\rho^S(r,t)$ and $\rho^I(r,t)$, which are solutions of the following diffusion-reaction equations:

$$\frac{\partial \rho^S(r,t)}{\partial t} = \hat{L}^S(r)\, \rho^S(r,t) - W_{CS}(r)\, \rho^S(r,t) \tag{1}$$

$$\frac{\partial \rho^I(r,t)}{\partial t} = W_{CS}(r)\, \rho^S(r,t)\, P^S(t) + \hat{L}^I(r)\, \rho^I(r,t) - W_R(r)\, \rho^I(r,t) \tag{2}$$

where $\hat{L}^S(r)$ and $\hat{L}^I(r)$ are diffusion operators for neutral and ionic species, and $W_{CS}(r)$ and $W_R(r)$ are the reaction probabilities for charge separation and recombination at intrapair distance r. The populations are related to these pair distribution functions as follows:

$$P^S(t) = \exp\left(-\frac{t}{\tau_S} - c\int_0^t k(t')\,dt'\right) \quad \text{with}$$

$$k(t) = 4\pi \int_\sigma^\infty r^2 W_{CS}(r)\, \rho^S(r,t)\, dr \tag{3}$$

$$P^I(t) = 4\pi c \int_\sigma^\infty r^2 \rho^I(r,t)\, dr \tag{4}$$

where τ_S is the lifetime of $^1Pe^*$ without quencher, c is the quencher concentration, and σ is the contact distance. Directly after excitation, the reactant pair distribution is essentially independent of r, except at close to contact distances, where it is influenced by the molecular nature of the solvent. CS occurs first in reactant pairs at optimal distance/orientation, i.e., without significant diffusion. Afterward, $\rho^S(r,t)$ exhibits a "hole" at short distances and CS becomes slower because it occurs at larger distances and/or diffusion is required. Therefore, the rate coefficient, $k(t)$, in eq 3 is time dependent and decreases from its static-quenching limit to its diffusion-controlled limit. The same principles apply for the ion-pair distribution function, with the important distinction that it differs strongly from $\rho^S(r,t)$ as it is determined by the CS step (first term of the right-hand side of eq 2). Thus, ion-pair dynamics are intrinsically non-Markovian.

Although singlet and triplet ion pairs cannot be differentiated in the TA experiments, their pair distributions, $\rho^{IS}(r,t)$ and $\rho^{IT}(r,t)$, were distinguished in the analysis and $W_R(r)$ was split into $W_{RS}(r)$ and $W_{RT}(r)$ to properly account for the singlet and triplet charge recombination pathways (Scheme 1). Finally, the reaction probabilities for charge separation and recombination, $W_x(r)$ (x = CS, RS, RT), were modeled using the semiclassical Marcus expression for nonadiabatic ET, accounting for its distance dependence through the electronic coupling, $V_x(r)$, the solvent reorganization energy, $\lambda_s(r)$, and the driving force, $\Delta G_x(r)$ (see Supporting Information).

Figures 2 and S8−13 reveal that the temporal evolution of the singlet excited-state, ion, and triplet excited-state populations can be well reproduced using this UET approach for both quenchers at all concentrations and in all three solvents, with the parameters listed in Table S1. For a given quencher, the data in ACN and DG17 could be simulated using the same set of parameters, apart from those associated with the solvent, namely, $\lambda_s(r)$, and the diffusion coefficients.

For EMIDCA, the same approach allowed reproducing $P^S(t)$, i.e., the CS step. However, this was only possible assuming a larger driving force and reorganization energy than those calculated for a solvent with a static dielectric constant ε_s = 11, as measured for EMIDCA.[49] This issue on the ability of ε_s to properly account for the effective polarity of RTILs is well-known.[25,50−52] However, simulations of $P^I(t)$ and $P^T(t)$ failed even when taking this effect into account. The profiles were essentially the same as in DG17, i.e., the free-ion yield was too small and the triplet yield too large.

The ionic nature of EMIDCA had to be accounted for to reproduce the data in this solvent. This was done by including in the model the screening of the Coulombic interaction between the photoproduced ions by the ionic solvent. The Coulombic interaction energy, C, enters the diffusion operator $\hat{L}^I(r)$ in eq 2 as well as the driving force for charge separation and recombination calculated with the Weller equation (eq S2).[53] It can be expressed using the Onsager radius, r_C:

$$C = k_B T \frac{r_C}{r} \qquad \text{with} \qquad r_C = \frac{\prod_i z_i e}{4\pi \varepsilon_0 \varepsilon_s k_B T} \qquad (5)$$

where $z_i e$ is the electric charge of the constituent i of the pair and the other symbols have their usual meaning. The Onsager radius corresponds to the intrapair distance at which the Coulombic interaction is equal to thermal energy. The presence of a salt leads to a screening of the Coulomb potential and, on the basis of the Debye–Hückel theory, the Onsager radius can be expressed as[48,54]

$$r'_C = \frac{r_C}{(1 + \sigma/\Lambda)} \exp\left(\frac{\sigma - r}{\Lambda}\right) \qquad (6)$$

where the Debye screening length, Λ, scales with the inverse square root of the ionic strength (eq S10).

Although Debye–Hückel theory is not strictly valid at high ionic concentrations, this modified Onsager radius, r'_C, allows for a qualitative estimate of the effect of the screening on the ion-pair dynamics. Increasing ionic strength decreases Λ and, thus, the Onsager radius. High salt concentrations, >1 M, lead to Onsager radii of a few angstroms only. Therefore, this suggests a quasi suppression of the Coulombic interaction within the ion pair in RTILs. In this respect, the ions behave as if they were neutral species. Although the Coulombic interaction is negligible, the ions should still be considered as paired as long as their recombination is geminate, namely, as long as the probability of reencounter is larger than that of encountering an ion born from another pair. According to our results, this is the case up to several hundreds of nanoseconds in EMIDCA (Figure 2).

This screening also affects the driving forces for charge separation and recombination. However, as mentioned above, the Weller equation seems not to properly account for the effective driving force in RTILs. Despite this, the screening should almost suppress the distance dependence of the driving force, as shown in Figure S16. In the case of charge recombination, Coulomb stabilization results in a smaller driving force at short distance. As charge recombination to the ground state occurs in the inverted region, this should accelerate recombination. Because of the screening, this effect is expected to be much less pronounced in RTILs than in conventional solvents.

The good agreement between the measured population dynamics and those simulated with UET including the modified Onsager radius, r'_C, suggests that the differences observed between EMIDCA and DG17 arises from the screening of the electrostatic interaction in the ion pair by the ionic solvent. In EMIDCA, the ions have to overcome a significantly smaller barrier for escaping than in DG17 and, thus, Φ_I is larger. Similarly, the smaller Φ_T is also consistent with a smaller Coulomb potential, because triplet charge recombination requires the reencounter of ions after their diffusion to a distance where spin conversion is operative. Although escape and, thus, spin conversion are facilitated in EMIDCA, triplet recombination is less efficient than in DG17 because of the weaker attractive forces.

In conclusion, our investigation reveals that, whereas the ionic nature of RTILs has a minor effect on the dynamics of photoinduced charge separation, it has a significant impact on the dynamics of the ensuing ions. Indeed, it enhances the generation of free ions, contrary to what could be concluded from previous investigations where the RTILs were not compared with dipolar solvents of the same viscosity. Our analysis, based on a diffusion-reaction model, suggests that this arises mostly from the screening of the electrostatic potential within the photogenerated ion pair by the solvent ions. As a consequence, the escape from the ion pair is facilitated. In this respect, this is similar to the special salt effect observed in conventional solvents.[34−39] Unfortunately, this advantageous feature of RTILs is counterbalanced by their high viscosity, which inhibits high free ion yields. However, working at higher temperatures, where viscosity is significantly lower, could circumvent, at least partially, this limitation.

■ ASSOCIATED CONTENT

Ⓢ Supporting Information

The Supporting Information is available free of charge on the ACS Publications website at DOI: 10.1021/acs.jp-clett.8b03030.

> Experimental details (including tables of quencher concentrations and solvent properties), TA, absorption, and difference spectra, kinetic graphs, details on the diffusion−reaction model (including graphs of the distance dependence of the Coulomb potential and a table of electron transfer parameters), list of symbols (PDF)

■ AUTHOR INFORMATION

Corresponding Authors

*G. Angulo. E-mail: gangulo@ichf.edu.pl.
*E. Vauthey. E-mail: Eric.Vauthey@unige.ch.

ORCID Ⓘ

Arnulf Rosspeintner: 0000-0002-1828-5206
Marius Koch: 0000-0001-8721-7613
Gonzalo Angulo: 0000-0002-6484-1795
Eric Vauthey: 0000-0002-9580-9683

Present Address

§Solvias AG, Römerpark 2, 4303 Kaiseraugst, Switzerland.

Notes

The authors declare no competing financial interest.

■ REFERENCES

(1) Welton, T. Room-Temperature Ionic Liquids. Solvents for Synthesis and Catalysis. *Chem. Rev.* **1999**, *99*, 2071−2084.
(2) Plechkova, N. V.; Seddon, K. R. Applications of Ionic Liquids in the Chemical Industry. *Chem. Soc. Rev.* **2008**, *37*, 123−150.
(3) Hallett, J. P.; Welton, T. Room-Temperature Ionic Liquids: Solvents for Synthesis and Catalysis. 2. *Chem. Rev.* **2011**, *111*, 3508−3576.
(4) Watanabe, M.; Thomas, M. L.; Zhang, S.; Ueno, K.; Yasuda, T.; Dokko, K. Application of Ionic Liquids to Energy Storage and Conversion Materials and Devices. *Chem. Rev.* **2017**, *117*, 7190−7239.

(5) Alvaro, M.; Ferrer, B.; Garcia, H.; Narayana, M. Screening of an Ionic Liquid as Medium for Photochemical Reactions. *Chem. Phys. Lett.* **2002**, *362*, 435−440.

(6) Pagni, R. M.; Gordon, C. M. Photochemistry in Ionic Liquids. *CRC Handbook of Organic Photochemistry and Photobiology*, 2nd ed.; CRC Press, 2004; pp 5/1−21.

(7) Weingärtner, H. Understanding Ionic Liquids at the Molecular Level: Facts, Problems, and Controversies. *Angew. Chem., Int. Ed.* **2008**, *47*, 654−670.

(8) Castner, E. W.; Wishart, J. F. Spotlight on Ionic Liquids. *J. Chem. Phys.* **2010**, *132*, 120901.

(9) Samanta, A. Solvation Dynamics in Ionic Liquids: What We Have Learned from the Dynamic Fluorescence Stokes Shift Studies. *J. Phys. Chem. Lett.* **2010**, *1*, 1557−1562.

(10) Castner, E. W.; Margulis, C. J.; Maroncelli, M.; Wishart, J. F. Ionic Liquids: Structure and Photochemical Reactions. *Annu. Rev. Phys. Chem.* **2011**, *62*, 85−105.

(11) Garcia, H.; Navalon, S. Photochemistry in Ionic Liquids. *RSC Catal. Ser.* **2014**, *15*, 474−507.

(12) Aster, A.; Vauthey, E. More than a Solvent: Donor-Acceptor Complexes of Ionic Liquids and Electron Acceptors. *J. Phys. Chem. B* **2018**, *122*, 2646−2654.

(13) Bixon, M.; Jortner, J. Electron Transfer-from Isolated Molecules to Biomolecules. *Adv. Chem. Phys.* **2007**, *106*, 35−202.

(14) Balzani, V. *Electron Transfer in Chemistry*; J. Wiley: New York, 2001.

(15) Rosspeintner, A.; Vauthey, E. Bimolecular Photoinduced Electron Transfer Reactions in Liquids under the Gaze of Ultrafast Spectroscopy. *Phys. Chem. Chem. Phys.* **2014**, *16*, 25741−25754.

(16) Banerji, N.; Angulo, G.; Barabanov, I. I.; Vauthey, E. Intramolecular Charge-Transfer Dynamics in Covalently Linked Perylene-Dimethylaniline and Cyanoperylene-Dimethylaniline. *J. Phys. Chem. A* **2008**, *112*, 9665−9674.

(17) Lee, H. Y.; Issa, J. B.; Isied, S. S.; Castner, J.; Edward, W.; Pan, Y.; Hussey, C. L.; Lee, K. S.; Wishart, J. F. A Comparison of Electron-Transfer Dynamics in Ionic Liquids and Neutral Solvents. *J. Phys. Chem. C* **2012**, *116*, 5197−5208.

(18) Santhosh, K.; Samanta, A. What Determines the Rate of Excited-State Intramolecular Electron-Transfer Reaction of 4-(N,N-dimethylamino)benzonitrile in Room Temperature Ionic Liquids? A Study in [bmim][PF6]. *ChemPhysChem* **2012**, *13*, 1956−1961.

(19) Muramatsu, M.; Katayama, T.; Ito, S.; Nagasawa, Y.; Matsuo, D.; Suzuma, Y.; Peng, L.; Orita, A.; Otera, J.; Miyasaka, H. Photoinduced Charge-Transfer Dynamics of Sequentially Aligned Donor-Acceptor Systems in an Ionic Liquid. *Photochem. Photobiol. Sci.* **2013**, *12*, 1885−1894.

(20) Muramatsu, M.; Morishima, S.; Katayama, T.; Ito, S.; Nagasawa, Y.; Miyasaka, H. The Effect of Pre-solvation in the Ground State on Photoinduced Electron Transfer in Ionic Liquids. *J. Solution Chem.* **2014**, *43*, 1550−1560.

(21) DeVine, J. A.; Labib, M.; Harries, M. E.; Rached, R. A. M.; Issa, J.; Wishart, J. F.; Castner, E. W. Electron-Transfer Dynamics for a Donor-Bridge-Acceptor Complex in Ionic Liquids. *J. Phys. Chem. B* **2015**, *119*, 11336−11345.

(22) Sahu, P. K.; Das, S. K.; Sarkar, M. Studies on Intramolecular electron transfer reaction in donor-spacer-acceptor systems in room-temperature ionic liquids. *J. Mol. Liq.* **2016**, *214*, 24−31.

(23) Ando, R. A.; Brown-Xu, S. E.; Nguyen, L. N. Q.; Gustafson, T. L. Probing the Solvation Structure and Dynamics in Ionic Liquids by Time-Resolved Infrared Spectroscopy of 4-Dimethylamino benzonitrile. *Phys. Chem. Chem. Phys.* **2017**, *19*, 25151−25157.

(24) Kimura, Y.; Ibaraki, S.; Hirano, R.; Sugita, Y.; Yasaka, Y.; Ueno, M. Photoexcitation Dynamics of p-Nitroaniline and N,N-Dimethyl-p-nitroaniline in 1-Alkyl-3-methylimidazolium-Cation Based Ionic Liquids with Different Alkyl-Chain Lengths. *Phys. Chem. Chem. Phys.* **2017**, *19*, 22161−22168.

(25) Liang, M.; Kaintz, A.; Baker, G. A.; Maroncelli, M. Bimolecular Electron Transfer in Ionic Liquids: Are Reaction Rates Anomalously High? *J. Phys. Chem. B* **2012**, *116*, 1370−1384.

(26) Koch, M.; Rosspeintner, A.; Angulo, G.; Vauthey, E. Bimolecular Photoinduced Electron Transfer in Imidazolium-Based Room-Temperature Ionic Liquids Is Not Faster than in Conventional Solvents. *J. Am. Chem. Soc.* **2012**, *134*, 3729−3736.

(27) Wu, B.; Liang, M.; Maroncelli, M.; Castner, E. W. Photoinduced Bimolecular Electron Transfer from Cyano Anions in Ionic Liquids. *J. Phys. Chem. B* **2015**, *119*, 14790−14799.

(28) Wu, B.; Maroncelli, M.; Castner, E. W. Photoinduced Bimolecular Electron Transfer in Ionic Liquids. *J. Am. Chem. Soc.* **2017**, *139*, 14568−14585.

(29) Wu, B.; Liang, M.; Zmich, N.; Hatcher, J.; Lall-Ramnarine, S. I.; Wishart, J. F.; Maroncelli, M.; Castner, J.; Edward, W. Photoinduced Bimolecular Electron Transfer in Ionic Liquids: Cationic Electron Donors. *J. Phys. Chem. B* **2018**, *122*, 2379−2388.

(30) Masnovi, J. M.; Kochi, J. K. Direct Observation of Ion Pair Dynamics. *J. Am. Chem. Soc.* **1985**, *107*, 7880−7893.

(31) Peters, K. S.; Lee, J. Picosecond Dynamics of Stilbene-Olefin Contact and Solvent Separated Radical Ion Pairs: Role of Electron Transfer and Radical Ion Pair Diffusion. *J. Am. Chem. Soc.* **1993**, *115*, 3643−3646.

(32) Gould, I. R.; Farid, S. Dynamics of Bimolecular Photoinduced Electron Transfer Reactions. *Acc. Chem. Res.* **1996**, *29*, 522−528.

(33) Mataga, N.; Miyasaka, H. Electron Transfer and Exciplex Chemistry. *Adv. Chem. Phys.* **2007**, *107*, 431−496.

(34) Mizuno, K.; Ichinose, N.; Otsuji, Y. The Cis-Trans Photo-isomerization and Photooxygenation of 1,2-Diarylcyclopropanes. Salt Effects on the Photoinduced Electron Transfer Reactions. *Chem. Lett.* **1985**, *14*, 455−458.

(35) Goodson, B.; Schuster, G. B. Salt Effects in Photoinduced Electron-Transfer Reactions. *Tetrahedron Lett.* **1986**, *27*, 3123−6.

(36) Yabe, T.; Kochi, J. K. Contact ion pairs. Picosecond Dynamics of Solvent Separation, Internal Return, and Special Salt Effect. *J. Am. Chem. Soc.* **1992**, *114*, 4491−4500.

(37) Grosso, V. N.; Previtali, C. M.; Chesta, C. A. Salt-Induced Charge Separation in Photoinduced Electron Transfer Reactions. The Effect of Ion Size. *Photochem. Photobiol.* **1998**, *68*, 481−486.

(38) Sun, D.; Hubig, S. M.; Kochi, J. K. Electron-Transfer Pathway for Photoinduced Diels-Alder Cycloadditions. *J. Photochem. Photobiol., A* **1999**, *122*, 87−94.

(39) Winstein, S.; Klinedinst, P. E.; Robinson, G. C. Salt Effects and Ion Pairs in Solvolysis and Related Reactions. XVII. Induced Common Ion Rate Depression and the Mechanism of the Special Salt Effect. *J. Am. Chem. Soc.* **1961**, *83*, 885−895.

(40) Paul, A.; Samanta, A. Photoinduced Electron Transfer Reaction in Room Temperature Ionic Liquids: A Combined Laser Flash Photolysis and Fluorescence Study. *J. Phys. Chem. B* **2007**, *111*, 1957−1962.

(41) Yago, T.; Ishii, Y.; Wakasa, M. Diffusion and Solvation of Radical Ions in an Ionic Liquid Studied by the MFE Probe. *J. Phys. Chem. C* **2014**, *118*, 22356−22367.

(42) Angulo, G.; Brucka, M.; Gerecke, M.; Grampp, G.; Jeannerat, D.; Milkiewicz, J.; Mitrev, Y.; Radzewicz, C.; Rosspeintner, A.; Vauthey, E.; et al. Characterization of Dimethylsulfoxide/Glycerol Mixtures: a Binary Solvent System for the Study of "Friction-Dependent" Chemical Reactivity. *Phys. Chem. Chem. Phys.* **2016**, *18*, 18460−18469.

(43) Lang, B.; Mosquera-Vazquez, S.; Lovy, D.; Sherin, P.; Markovic, V.; Vauthey, E. Broadband Ultraviolet-Visible Transient Absorption Spectroscopy in the Nanosecond to Microsecond Time Domain with Sub-Nanosecond Time Resolution. *Rev. Sci. Instrum.* **2013**, *84*, 073107−8.

(44) Angulo, G.; Rosspeintner, A.; Lang, B.; Vauthey, E. Optical Transient Absorption Experiments Reveal the Failure of Formal Kinetics in Diffusion Assisted Electron Transfer Reactions. *Phys. Chem. Chem. Phys.* **2018**, *20*, 25531−25546.

(45) Marcus, R. A.; Sutin, N. Electron Transfer in Chemistry and Biology. *Biochim. Biophys. Acta, Rev. Bioenerg.* **1985**, *811*, 265−322.

(46) Pages, S.; Lang, B.; Vauthey, E. Ultrafast Excited State Dynamics of the Perylene Radical Cation Generated upon

Bimolecular Photoinduced Electron Transfer Reaction. *J. Phys. Chem. A* **2006**, *110*, 7547−7553.

(47) Steiner, U. E.; Ulrich, T. Magnetic Field Effects in Chemical Kinetics and Related Phenomena. *Chem. Rev.* **1989**, *89*, 51−147.

(48) Burshtein, A. Unified Theory of Photochemical Charge Separation. *Adv. Chem. Phys.* **2007**, *114*, 419−587.

(49) Hunger, J.; Stoppa, A.; Schrödle, S.; Hefter, G.; Buchner, R. Temperature Dependence of the Dielectric Properties and Dynamics of Ionic Liquids. *ChemPhysChem* **2009**, *10*, 723−733.

(50) Lynden-Bell, R. M. Redox Potentials and Screening in Ionic Liquids: Effects of Sizes and Shapes of Solute Ions. *J. Chem. Phys.* **2008**, *129*, 204503.

(51) Kobrak, M. N.; Li, H. Electrostatic Interactions in Ionic Liquids: the Dangers of Dipole and Dielectric Descriptions. *Phys. Chem. Chem. Phys.* **2010**, *12*, 1922−1932.

(52) Lee, H. Y.; Issa, J. B.; Isied, S. S.; Castner, E. W.; Pan, Y.; Hussey, C. L.; Lee, K. S.; Wishart, J. F. A Comparison of Electron-Transfer Dynamics in Ionic Liquids and Neutral Solvents. *J. Phys. Chem. C* **2012**, *116*, 5197−5208.

(53) Weller, A. Photoinduced Electron Transfer in Solutions: Exciplex and Radical Ion Pair Formation Free Enthalpies and their Solvent Dependence. *Z. Phys. Chem.* **1982**, *133*, 93−98.

(54) Kornyshev, A. A. Non-local Dielectric Response of a Polar Solvent and Debye Screening in Ionic Solution. *J. Chem. Soc., Faraday Trans. 2* **1983**, *79*, 651−661.